

The Cosmic Ray spectrum in the energy region between 10^{12} and 10^{16} eV measured by ARGO–YBJ

Paolo Montini^{1,a} for the ARGO–YBJ collaboration

¹*Dipartimento di Matematica e Fisica - Università degli Studi Roma TRE and INFN Sezione di Roma TRE*

Abstract. The ARGO-YBJ experiment has been in full and stable data taking at the Yangbajing cosmic ray observatory (Tibet, P.R. China, 4300 m a.s.l.) for more than five years. The detector has been designed in order to explore the Cosmic Ray (CR) spectrum in an energy range from few TeV up to several PeV. The high segmentation of the detector allows a detailed measurement of the lateral particle distribution which can be exploited in order to identify showers produced by primaries of different mass. The results of the measurement of the all-particle and proton plus helium energy spectra in the energy region between 10^{12} and 10^{16} eV are discussed.

The measurement of Cosmic Ray (CR) energy spectrum and composition gives important information concerning the production, acceleration and the propagation of high energy particles in our Galaxy. The CR all-particle energy spectrum is roughly described by a power-law with a *knee* at energies around 3 PeV. It is commonly believed that the origin of the knee is related to a change of the elemental composition of CRs, in particular to a decrease of the flux of light elements (H and He nuclei). The determination of the individual abundances of elements at energies above 100 TeV must be inferred from the measurements of extensive air showers (EAS). The development of EASs is subject to large fluctuations. Owing to the high altitude location (atmospheric depth 606 g/cm^2), the ARGO-YBJ experiment is able to sample the EAS induced by high energy CRs not far from the maximum of its longitudinal development where the fluctuations are reduced.

1 The detector

The ARGO–YBJ experiment was a full-coverage EAS detector operated at the Yangbajing cosmic ray observatory (Tibet, P.R. China, 4300 m a.s.l.) and it was in full and stable data taking from November 2007 up to February 2013. The detector was made of a single layer of 1836 Resistive Plate Chambers (RPCs) with $\sim 93\%$ active area surrounded by a partially instrumented ($\sim 23\%$) guard ring in order to improve the event reconstruction. The detector was equipped with two independent readout systems: each RPC is simultaneously read-out by 80 copper strips ($6.75 \times 61.80 \text{ cm}^2$) logically arranged in 10 independent pads ($55.6 \times 61.8 \text{ cm}^2$) and by two large electrodes called Big Pads ($139 \times 123 \text{ cm}^2$). Each Big Pad collects the total charge developed by the particles impinging on the detector surface (analog readout) [1]. The analog readout system can be operated at different gain scales in order to measure showers induced by primaries in a wide energy region. Data coming from the most sensitive

^aNow at Dipartimento di Fisica - Sapienza Università di Roma and INFN sezione di Roma e-mail: paolo.montini@roma1.infn.it

scales perfectly overlap with the digital readout, thus providing a powerful inter-calibration [1]. At the highest scale the analog readout samples the shower front up to a particle density of $2 \cdot 10^4 \text{ m}^{-2}$, thus extending the dynamic range of the detector up to PeV energies. A dedicated calibration procedure has been implemented for each gain scale [1, 2]. The full-coverage technique enables a detailed imaging of the shower front which is a fundamental tool that allows a deep investigation of the shower properties even in the core region. The high segmentation of the Big Pad system allows the measurement of the shower size and of the lateral distribution of particles in the shower front that can be exploited in order to estimate the primary energy and mass.

2 Data Analysis

The analysis has been carried out on events collected during 2010 by using the analog readout system. For each event the core position, arrival direction, shower size (N_8), particle density on the carpet and lateral distribution are reconstructed. The shower size N_8 has been defined as the number of particles within a radius of 8 m from the shower core. It is well correlated with energy for a given mass and not affected by bias effects due to the finite detector size [3]. The determination of the energy and of the primary mass from the measured quantities can be faced out by using the Bayesian unfolding. The Monte Carlo simulations are therefore used in order to evaluate a probabilistic response matrix which can be inverted by means of an iterative algorithm based on the Bayes's theorem. A detailed description of this procedure can be found in [4–6]. Showers produced by H, He, CNO, NeMgSi, and Fe have been simulated in the energy range $1 - 31.6 \times 10^4 \text{ TeV}$ with an E^{-1} differential spectrum by using the CORSIKA (v. 7.3) code [7] including the QGSJET-II.04 and FLUKA interaction models. A smaller data set have been simulated using SYBILL 2.1 for systematic studies. Showers have been sampled at the Yangbajing altitude and randomly distributed over an area of $250 \times 250 \text{ m}^2$ centered on the ARGO-YBJ detector. The detector response has been simulated by using a GEANT3 based code. The present analysis is based on the data collected with two analog scales (low gain and high gain) covering the energy range from about 20 TeV to a few PeV. A sample of quasi-vertical showers ($\vartheta_{rec} \leq 35^\circ$) has been selected within an area of $40 \times 40 \text{ m}^2$ around the detector center ensuring that a large fraction of the shower is fully contained in the full-coverage area. Additional selection criteria based on the shower size improve the correlation between shower size and primary energy and avoid any contribution due to the electronic noise. In figure 1a the shower size N_8 of data and MC events is reported, showing a good agreement between data and simulations. In figure 1b the selection efficiency is shown for proton, helium nuclei, CNO and NeMgSi mass groups and iron nuclei. The plot shows that in the energy region 300 TeV – 10 PeV the selection efficiency is almost the same for all the species, demonstrating the selection criteria do not affect the spectrum measurement.

In a shower produced by heavy nuclei a substantial amount of secondary particles is spread further away from the core region. On the contrary, in a shower produced by light elements, the largest amount of particles is concentrated in a small region around the shower core. The ratio between the particle density measured at several distances from the core and the one measured very close to the core can be exploited in order to identify showers produced by light elements. Several studies performed on simulated events have shown that the quantities $\beta_5 = \rho_5/\rho_0$, and $\beta_{10} = \rho_{10}/\rho_0$, where ρ_0 , ρ_5 and ρ_{10} are respectively the particle density measured in the core region, at 5 m from the core and at 10 m from the core, are sensitive to primary mass. In a probabilistic approach the probability $P(N_8, \beta_5, \beta_{10}|E, A)$ of measuring a shower size N_8 and a certain value of β_5 and β_{10} giving a primary energy E and mass A , relates the characteristics of the primary particle to the experimental observables. The bayesian unfolding algorithm has been therefore tuned in order to take into account also the information coming from the two quantities β_5 and β_{10} . The fraction of selected showers induced by light elements (p and

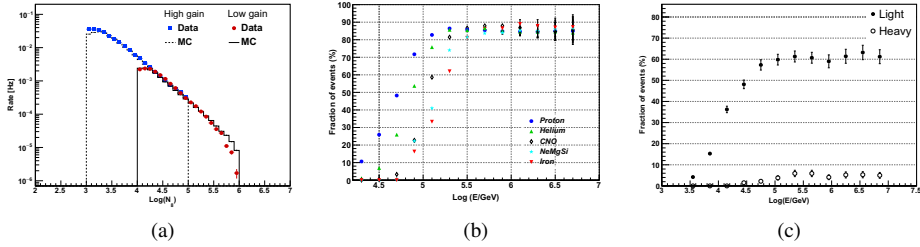


Figure 1: Shower size distribution for data and simulations (a), Fraction of selected MC showers produced by P, He, CNO, NeMgSi and Fe(b). Fraction of selected MC showers produced by light elements and the corresponding contamination

He) and the corresponding contamination by heavier nuclei has been evaluated in order to check the discrimination power. In figure 1c the values obtained are reported as a function of the energy. The fraction of selected light elements increases with energy and is around 60% at energies above 50 TeV, while contamination is well below 10% over the whole energy range.

3 All-particle and P+He energy spectra

In the figure 2a the all-particle spectrum measured in this work is reported. The measurements are affected by a statistical uncertainty of the order of 1% at the lowest energies, gradually increasing up to $\sim 8\%$ at energies higher than 1 PeV. The systematic uncertainty is of the order of 15% mainly due to the limited Monte Carlo statistics (10%) and to variations of the bin edges (10%) used in the determination of the probability response matrix. The systematic uncertainty related to the hadronic interaction model used in simulations has been derived by comparing the results obtained by QGSJET and SIBYLL. In particular, simulations with SIBYLL systematically yield to a flux $\sim 7\%$ higher. Systematic effects introduced by variation of the fiducial cuts and by the unfolding procedure have also been studied and give a minor contribution ($\leq 1\%$) to the total uncertainty.

The proton plus helium spectrum, including both statistical and systematic errors is also reported in figure 2a, spanning the energy range between 20 TeV and 5 PeV. Statistical errors are of the order of 1% at the lowest energies and increase with energy up to 18% at PeV energies. The contributions to the total systematic uncertainty come from event selection, estimation of the conditional probabilities, hadronic interaction model, composition model, unfolding procedure. As for the all-particle spectrum the major contribution to the systematic uncertainty comes from the determination of the probability response matrix and is about 10% for energy below 300 TeV, 8% in the region 300–500 TeV and it turns to about 21% at the PeV energies. A minor contribution comes from the selection criteria (2.5%) and the unfolding procedure ($\leq 1\%$). Simulations with SIBYLL yield to a flux $\sim 4\%$ and $\sim 10\%$ higher in the energy region below and above 500 TeV respectively.

4 Conclusions

The ARGO-YBJ experiment allows a deep investigation of the properties of EASs providing a detailed measurement of the distribution of the charged particles in the shower front. The detector is able to investigate the CR energy spectrum in a wide energy range. The measurements of the

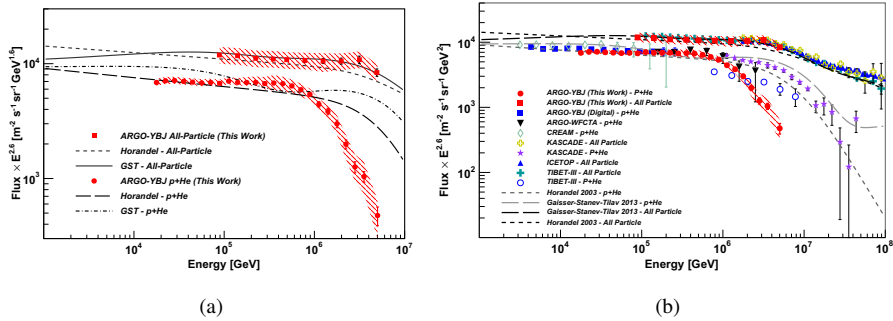


Figure 2: CR all-particle and p+He energy spectra measured by ARGO-YBJ (a) compared with previous results of ARGO-YBJ [6, 8], other experimental results [9] and theoretical models [10] (b).

all-particle and p+He energy spectra are presented. As shown in figure 2b the all-particle spectrum is in good agreement with other experimental results [9]. The measurement is also in agreement with an independent analysis of ARGO-YBJ data [11]. The accurate reconstruction of the lateral distribution has been exploited in order to discriminate showers produced by primaries of different mass groups. The ARGO-YBJ experiment measured the proton plus helium flux over two energy decades, from 3 TeV to 5 PeV. There is a strong evidence of a deviation from a single power law at energies around 1 PeV, suggesting that the *knee* of the all-particle spectrum is due to heavier elements. Similar conclusion has been suggested also by the results of the hybrid experiment ARGO-WFCTA based on a Wide FoV Cherenkov telescope. These results open new scenarios about the evolution of the p+He energy spectrum towards the highest energies and the origin of the knee.

References

- [1] B. Bartoli et al., *Astropart. Phys.* **67**, 47 (2015)
- [2] B. Bartoli et al., *Nucl. Instrum. Methods Phys. Res. Sect. A* **783**, 68 (2015)
- [3] P. Bernardini et al., *PoS(ICRC2015)388* (2015)
- [4] G. D'Agostini, *Nucl. Instrum. Meth.* **A362**, 487 (1995)
- [5] B. Bartoli et al., *Phys. Rev. D* **85**, 092005 (2012)
- [6] B. Bartoli et al., *Phys. Rev. D* **91**, 112017 (2015)
- [7] D. Heck, J. Knapp, J. Capdevielle, G. Schatz, T. Thouw, Report **FZKA 6019** (1998)
- [8] B. Bartoli et al., *Phys. Rev. D* **92**, 092005 (2015)
- [9] Y. S. Yoon et al., *ApJ* **728**, 122 (2011); T. Antoni et al., *Astroparticle Physics* **24**, 1 (2005); W. Apel et al., *Astropart. Phys.* **47**, 54 (2013); M. Amenomori et al., *Astrophys. J.* **678**, 1165 (2008); M.G. Aartsen et al., *Phys. Rev. D* **88**, 042004 (2013)
- [10] J.R. Hörandel, *Astropart. Phys.* **19**, 193 (2003), T.K. Gaisser et al. *Front. Phys.* **8(6)**, 748 (2013)
- [11] A. D'Amone et al., *PoS(ICRC2015)366*